Article

Acenaphthylene-Based Chromophores for Dye-Sensitized Solar Cells: Synthesis, Spectroscopic Properties, and Theoretical Calculations

Gabriela Malta, João Pina, J. Carlos Lima, A. Jorge Parola,* and Paula S. Branco*

Read Online

ACCESS | Metrics & More | Article Recommendations | SI Supporting Information

ABSTRACT: A set of acenaphthylene dyes with arylethynyl π-bridges was tested for dye-sensitized solar cells (DSSCs). Crucial steps for the extension of the conjugated system from the acenaphylene core involved Sonogashira coupling reactions. Phenyl, thiophene, benzotriazole, and thieno-[3,2-*b*]thiophene moieties were employed to extend the conjugation of the π-bridges. The systems were characterized by cyclic voltammetry and by UV−vis absorption and emission. The spectroscopic characterization showed that the last three bridges resulted in red-shifted absorption and emission spectra relative to the parent phenyl-bridged compound, in accordance with TD-DFT calculations. The phenylethynyl derivative **6a** achieved a conversion efficiency of 2.51% with V_{oc}, J_{sc}, and FF values of 0.365 V, 13.32 mA/cm^2, and 0.52, respectively. The efficiency of this compound improved to 3.15% with the addition of CDCA (10 mM), representing the best efficiency result in this study. The overall conversion efficiency of the other aryl derivatives **6b−d** proved to be significantly inferior (14−40%) to that of **6a** due to a significant decrease of J_{sc}.
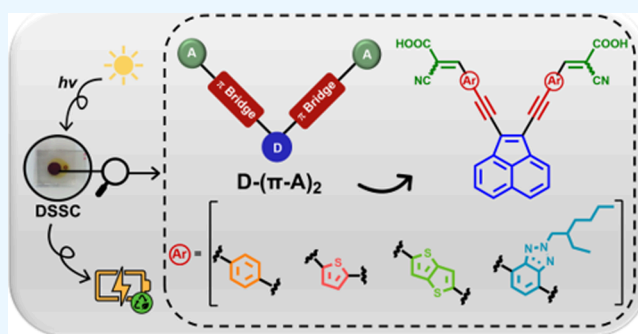
INTRODUCTION

The increase in energy consumption has led to further aggravation of environmental pollution and global warming. Among various renewable energy sources, solar energy presents several promising advantages and great potential for power generation. This carbon-free energy source is expected to play a prominent role in the achievement of carbon neutrality.[1,2] Some of these alternative technologies for energy conversion or storage are based in redox mediation processes that are at the core of many electrochemical devices, such as dye-sensitized solar cells (DSSCs).[3,4] The photovoltaic (PV) dye sensitized solar cell initially reported by O'Regan and Grätzel[5] represents one of the most interesting alternatives to the common silicon solar cells. This technology overcomes some of the many limitations of Si-based PV systems, such as their energy-intensive manufacturing methods, the poor conversion efficiency in low light intensities, and the relatively higher maintenance, driving the research to the last generation of PV cells, the dye-sensitized solar cells (DSSCs).[6,7] A DSSC device comprises a photoelectrode containing a dye adsorbed to a porous TiO$_2$ layer (anode), a counter electrode (cathode), and an electrolyte (redox mediator).[8] Despite the advancements made in these devices, their efficiencies remain lower than those of other competing technologies. The dye molecule (sensitizer) plays a crucial and central role in the DSSC with the design and synthesis of new organic molecules being the subject of intense study in the last 15 years.[3] Metal-free organic sensitizers have been quite investigated as an alternative to the highly efficient transition-metal complex sensitizers because they offer high flexibility in tuning the molecular architecture, high molar extinction coefficients, simpler and cheaper synthetic approaches, greater long-term chemical stability, and reduced environmental impact. Factors to be considered on the dye design include how effective it will be in light harvesting, electron injection, and dye regeneration, avoiding factors such as self-aggregation or back-recombination (charge recombination). The conventional architecture donor−π-bridge−acceptor (D−π−A) of the dyes has had many variations to increase the intramolecular charge transfer (ICT) through the push−pull effect (Figure 1).[9] As such, the dianchoring and dibranched groups of dyes, inspired by the architecture of the highly efficient ruthenium dyes, have emerged as a promising alternative (Figure 1).[10,11] This multibranched architecture presents advantages over the monobranched one, such as a greater structural variety to achieve panchromatic response, superior optical density conferred by the extended π-conjugated system, and increased
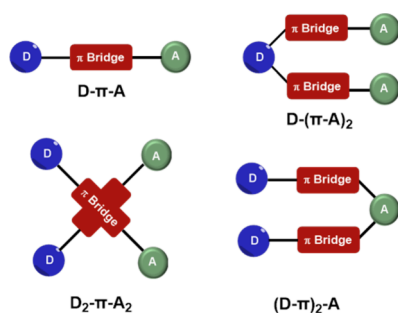
Figure 1. Schematic representation of the monobranched D−π−A architecture and typical multibranched multianchoring approach to organic DSSC dyes.

binding strength of the dye on the TiO$_2$ surface.[12,13] Polycyclic aromatic hydrocarbons (PAHs) encompass unique extended π-conjugated and planar structures widely present in compounds for application in diverse fields as organic field-effect transistors (OFETs),[14] organic light-emitting diodes (OLEDs),[15,16] organic photovoltaics (OPVs),[17] and DSSCs.[18,19]

Acenaphthylene is a PAH that has been widely used as a building block of several π-conjugated functional materials[17] such as bistriphenylamine fluoranthenes,[20] acenaphthopyrazines,[21] and acenaphthoBODIPYs.[22] Although having been employed in various materials, dyes containing an acenaphthylene as the main core have remained unexplored for the application on DSSCs when compared with other PAHs-based dyes such as biphenyl,[23,24] fluorene,[25,26] and anthracene.[27,28] To explore the potential of dyes with this central core in DSSCs, a new set of novel compounds containing a 1,2-diethynylacenaphthylene backbone with a D−(π−A)$_2$ dibranched and dianchoring architecture was synthesized (Figure 2).

By applying our knowledge on the synthesis of coumarin-based dyes,[29] here we report four new acenaphthylene-based dyes employing as π-bridges the phenyl, thiophene, benzotriazole, and thieno-[3,2-b]thiophene rings. it is expected that these different π-spacers could tune the absorption spectra and the photovoltaic performance of DSSCs. Cyanoacrylic acid, given its already reported ability,[30] was selected to be the anchoring group to TiO$_2$. The compounds have been applied in DSSC devices, and their performance was evaluated by measuring the current−voltage curves (I−V). Spectroscopic and electrochemical characterization of the compounds was also performed. The optimized geometry of the molecules was obtained through density functional theory (TD-DFT) studies.

RESULTS AND DISCUSSION

Synthesis. The synthetic pathway to obtain the 1,2 diethynylacenaphthylene-based dyes is summarized in Scheme 1. The tribromination of acenaphthene (**1**) by NBS followed by elimination of HBr allowed 1,2-dibromoacenaphthylene (**2**) to be obtained.[31,32] The phenyl dialdehyde derivative (**3a**) was readily prepared by a Sonogashira coupling reaction among 1,2-dibromoacenaphthylene (**2**) with 4-ethynylbenzaldehyde. To synthesize aldehydes **3b−d**, an alternative route was followed. The ethynyltrimethylsilane derivative **4** was obtained from **2** followed by the trimethylsilyl protecting groups' removal with K$_2$CO$_3$ in the presence of methanol, and the ethynyl intermediate was directly used in a coupling reaction with three different bromo aryl aldehydes (**5b−d**), as described in our previously reported method.[29] The bromo aryl aldehyde **5b** was commercial, but **5c** and **5d** were first prepared in the laboratory. In the case of **5c**, benzotriazole was alkylated with bromo-2-ethylhexane and then brominated.[33] The final step involved a formylation reaction with n-BuLi and DMF also used with 5-dibromothieno-[3,2-b]thiophene to prepare 5-bromothieno-[3,2-b]-thiophene-2-carbaldehyde (**5d**). The final chromophores (**6a−d**) were obtained through a Knoevenagel condensation between cyanoacetic acid and the four aldehydes (**3a−d**) with obtained yields ranging from 50 to 80%.

Absorption and Fluorescence. The optical properties of each chromophore were studied by measuring the UV−vis absorption and emission spectra in DMF as solvent at room temperature (Figure 3, Table 1). The absorption spectra show two distinct absorption bands: a stronger band (30,000−60,000 M^{-1} cm^{-1}) in the region 351−407 nm corresponding to the π−π* transition of the conjugated system and a weaker band (7000−17500 M^{-1} cm^{-1}) in the region 486−521 nm related to the intramolecular charge transfer (ICT) transition between the donor and the acceptor moieties. The UV−vis spectra of **6b**, **6c**, and **6d** are red-shifted when compared with those of **6a**. This could be related to the fact that the phenyl ring may have a twisted conformation with respect to the acenaphthylene ring in the case of **6a**, leading to a less efficient conjugation in a D−(π−A)$_2$ system.[34,35] However, theoretical calculations at the level carried out in this work (see below) do not confirm this hypothesis. The large Stokes shifts between the absorption and the emission bands (2889−3321 cm^{-1}) indicate a charge transfer character present on these dyes.[36]

Electrochemical Characterization. The electrochemical properties of the synthesized compounds were studied by using cyclic voltammetry (Table 2, Figure 4). From the obtained onsets of reduction peaks, the values of LUMO energies were calculated following the equation E [eV] =
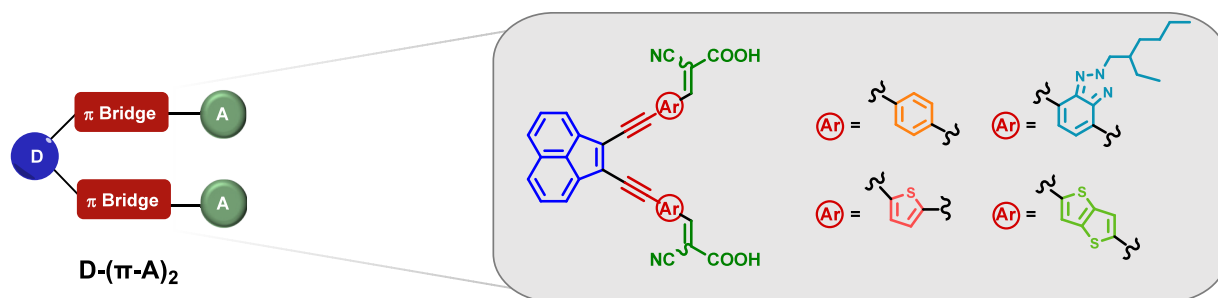
Figure 2. Schematic representation of a D−(π−A)$_2$ dye (donor, blue; π-bridge, red; acceptor, green). Structures of the synthesized and studied chromophores in this work.

Scheme 1. General Scheme for the Synthesis of 1,2-Diethynylacenaphthylene Dyes (6)[a]
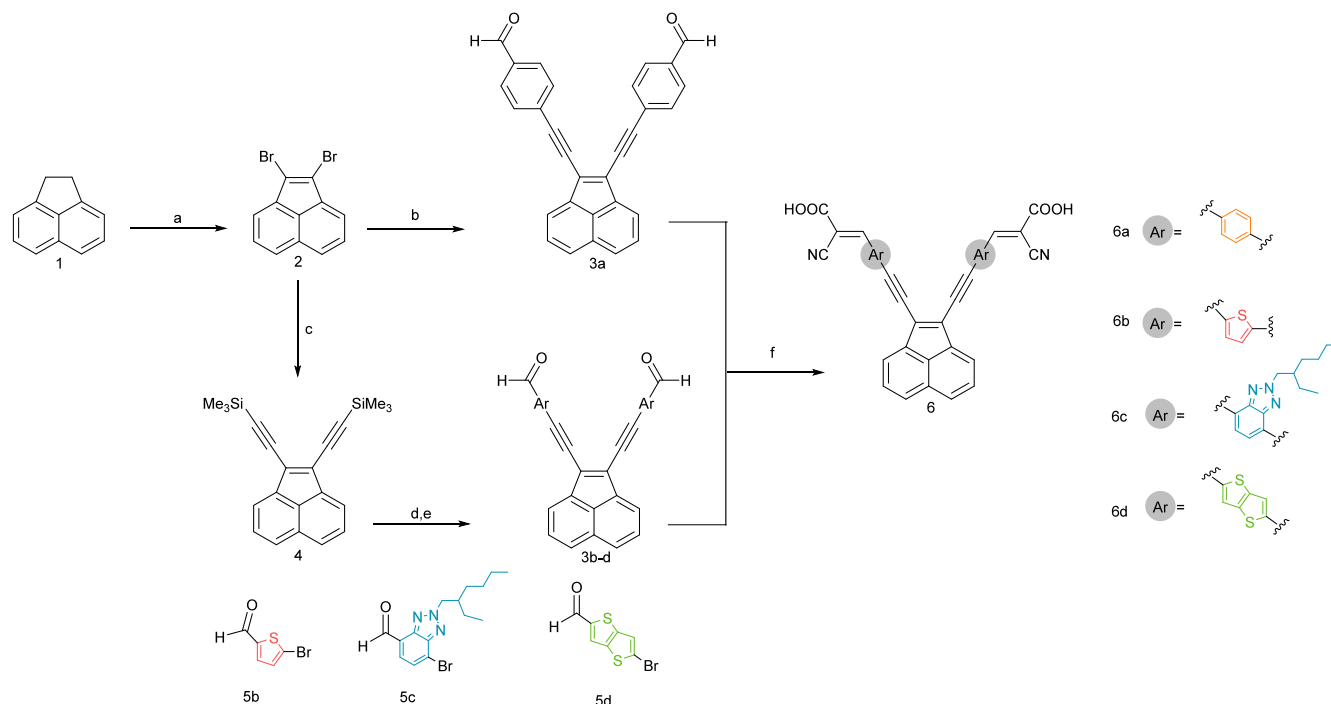
[a](a) 1 (1 equiv), NBS (3 equiv), benzoyl peroxide (0.1 equiv), CCl$_4$, reflux; (b) 2 (1 equiv), Pd(PPh$_3$)$_4$ (0.30 equiv), PPh$_3$ (0.12 equiv), CuI (0.24 equiv), 4-ethynylbenzaldehyde (3.0 equiv), DIPA (3 equiv), dry dioxane, 40°C in a degassed Schlenk tube; (c) 2 (1 equiv), Pd(PPh$_3$)$_4$ (0.30 equiv), PPh$_3$ (0.12 equiv), CuI (0.24 equiv), ethynyltrimethylsilane (3.0 equiv), DIPA (3 equiv), dry dioxane, 40°C in a sealed tube; (d) 4 (1 equiv), K$_2$CO$_3$ (2 equiv), dioxane/MeOH (1:1 v/v), RT; (e) Pd(PPh$_3$)$_4$ (0.20 equiv), PPh$_3$ (0.12 equiv), CuI (0.24 equiv), bromo aryl aldehydes (5b–d) (2.2 equiv), DIPA (2.0 equiv), dry dioxane, 40°C in a degassed Schlenk tube; and (f) 3a–d (1 equiv), cyanoacetic acid (6 equiv), piperidine (5.4 equiv), dry acetonitrile, reflux.
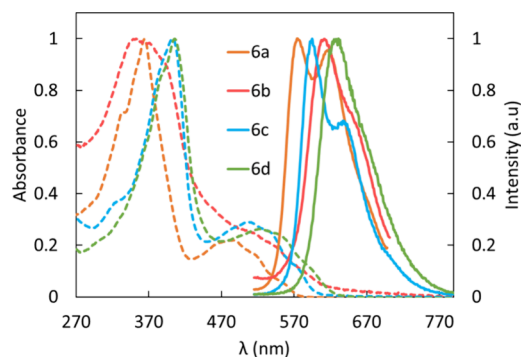
Figure 3. Normalized absorption (dotted) and fluorescence emission (solid; λ_{exc}(6a) = 364 and 486 nm; λ_{exc}(6b) = 351 nm; λ_{exc}(6c) = 402 and 507 nm; λ_{exc}(6d) = 407 and 521 nm spectra of chromophores 6a–d in DMF solution at room temperature (compounds excited at two different λ_{exc} have identical emission spectra)).

$-(E_{onset}$ (V vs SCE) + 4.44)[37] (Figure S27). The highest occupied molecular orbital energy levels, obtained from the LUMO energies and the energy from the optical transition

Table 2. Electrochemical Properties Obtained from Cyclic Voltammetry Measurements in Dimethylformamide (DMF) Solution with a Dye (6a–d) Concentration of 1.5 × 10^{-4} M and 0.1 M TBAPF$_6$ at Scan Rates of 50, 100, 250, and 500 mV s^{-1}

dye	E_{red} vs SCE (V)	LUMO vs vacuum (eV)	HOMO vs vacuum (eV)[a]	E_g (eV)[b]
6a	−0.83	−3.61	−5.90	2.29
6b	−0.69	−3.75	−5.95	2.21
6c	−0.60	−3.84	−6.04	2.21
6d	−0.77	−3.67	−5.79	2.13

[a]HOMO energy level determined from $E_{(HOMO)} = E_{(LUMO)} - E_g$.
[b]Energy gap (E_g) obtained from the intersection between the normalized absorption and fluorescence emission spectra (Figure 3).

(Table 2), are located between −6.04 and −5.79 eV, which are lower than the redox potential of the I$^-$/I$_3^-$ redox couple (−4.60 eV),[38] a condition that is required for efficient regeneration of the oxidized dye. The lowest occupied molecular orbital energy levels lie between −3.84 and −3.61

Table 1. Spectroscopic Data for the Synthesized Compounds (6a–d) in DMF Solution at Room Temperature (Absorption (λ_{abs}) and Emission (λ_{em}) Maxima, Molar Extinction Coefficients (ε), and Stokes Shift (ΔSS))

dye	λ_{abs1} (nm)	ε_1 (cm^{-1} M^{-1})	λ_{abs2} (nm)	ε_2 (cm^{-1} M^{-1})	λ_{em1} (nm)	λ_{em2} (nm)	ΔSS (cm^{-1})
6a	364	61,500	486	13,802	575	617	3185
6b	351	29,495	514 sh	7738	612		3115
6c	402	59,568	507	17,463	594	640	2889
6d	407	54,320	521	14,742	630		3321
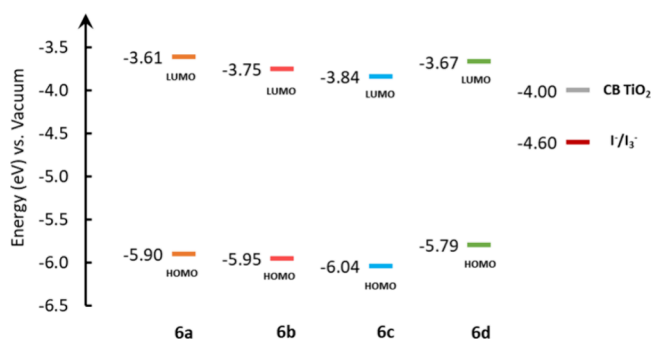
Figure 4. Schematic representation of the HOMO and LUMO energy levels of each chromophore vs the CB of TiO_2 and I^-/I_3^- redox potentials.

Figure 5. $I-V$ curves of the test cells based on the synthesized acenaphthylene dyes and reference N-719 under 100 mW cm^{-2} simulated AM 1.5 illumination (best performing cell, [CDCA] = 0 mM).

eV, which are higher than the CB of TiO_2 (-4.0 eV),[38] indicating that electron injection from the excited molecule to the CB of TiO_2 is energetically favorable.

Photovoltaic Performance. The efficiencies of the final 1,2-diethynylacenaphthylene chromophores (**6a–d**) were tested in DSSC devices, and the current–voltage curves ($I-V$) were measured. The photovoltaic parameters open-circuit voltage (V_{oc}), short-circuit current (J_{sc}), fill factor (FF), and photovoltaic conversion efficiency (η) and the $I-V$ curves are displayed, respectively, in Table 3 and Figure 5. The best performing dye was the derivative containing the phenyl bridge (**6a**) ($\eta = 2.51\%$), with V_{oc}, J_{sc}, and FF values 0.365 V, 13.32 mA/cm^2, and 0.52, respectively. The other derivatives (**6b–d**) presented lower efficiencies when compared to phenyl, with a significant decrease on J_{sc} (3.21–5.35 mA/cm^2) and also on V_{oc} (0.241–0.320 V). In our previous work with coumarin

dyes,[29] thieno-[3,2-b]thiophene has shown to be a very promising π-bridge due to its extended molecular conjugation, high stability, ring planarity, and S–S interactions.[39] The lower J_{sc} values of the more planar compounds could result from increased dye aggregation, where excited-state quenching could lead to inefficient electron injection into the CB of TiO_2 or from a more efficient electron hole recombination in the case of the more planar molecules.[40,41] To suppress eventual dye aggregation, chenodeoxycholic acid (CDCA) was used as coadsorbing agent. The effect of three different concentrations of CDCA (0, 10, and 50 mM) was explored (Table 3, Figure S28). The performance of the benzotriazole derivative (**6c**) in DSSCs increased linearly with the amount of CDCA, as well as the J_{sc} and V_{oc} values (Figure S29). The performance of this dye improved significantly from 0.44 to 1.78% (with 0 and 50 mM, respectively). It was expected that

Table 3. Performance Values of the Test Cells Based on the Synthesized Dyes and Reference Dye N-719 under 100 mW cm^{-2} AM 1.5 Illumination[a]

Dye	[CDCA]/mM	V_{oc}/V	J_{sc}/mA cm^{-2}	V_{max}/V	J_{max}/mA cm^{-2}	FF	η/%
6a	0	0.365±0.003	13.32±0.07	0.234±0.003	10.76±0.03	0.52±0.01	2.51±0.02
	10	0.404±0.008	13.62±0.6	0.274±0.003	11.39±0.5	0.57±0.02	3.15±0.1
	50	0.371±0.003	12.93±0.1	0.243±0.005	10.33±0.1	0.52±0.02	2.51±0.07
6b	0	0.241±0.007	3.21±0.2	0.157±0.004	2.24±0.2	0.45±0.01	0.35±0.02
	10	0.241±0.004	4.27±0.3	0.152±0.002	3.19±0.2	0.47±0.004	0.49±0.03
	50	0.240±0.007	3.39±0.2	0.155±0.002	2.50±0.1	0.48±0.03	0.39±0.02
6c	0	0.269±0.006	3.75±0.3	0.168±0.003	2.64±0.2	0.44±0.001	0.44±0.04
	10	0.287±0.006	4.70±0.3	0.175±0.003	3.66±0.2	0.47±0.001	0.65±0.04
	50	0.352±0.003	10.52±0.3	0.226±0.003	7.90±0.5	0.48±0.02	1.78±0.1
6d	0	0.320±0.005	5.35±0.1	0.225±0.01	4.42±0.1	0.58±0.06	1.00±0.09
	10	0.293±0.01	4.52±0.4	0.206±0.01	3.70±0.4	0.57±0.02	0.77±0.08
	50	0.291±0.004	4.67±0.2	0.206±0.005	3.90±0.1	0.59±0.02	0.80±0.01
N-719	0	0.442±0.02	16.10±0.07	0.294±0.004	13.28±0.1	0.55±0.02	3.90±0.07
	10	0.44±0.01	16.46±0.1	0.298±0.004	13.93±0.09	0.57±0.007	4.19±0.08
	50	0.46±0.01	14.59±0.7	0.310±0.01	12.44±0.4	0.58±0.03	3.86±0.05

[a]The results presented correspond to the average values of at least two cells per dye, each cell measured five times. Different concentrations of CDCA were applied (0, 10, and 50 mM). The prepared anodes were soaked for 16 h in a CH_2Cl_2/MeOH/H_2O 65:35:5 (% v/v) solution of the dye (0.5 mM) at room temperature in the dark. Electrolyte composition: 0.8 M LiI and 0.05 M I_2 in an acetonitrile/valeronitrile (85:15, % v/v).

the long and bulky ethylhexyl chains present in benzotriazole would prevent dye aggregation,[42] but apparently, this steric hindrance is not enough to disturb the existing $\pi\cdots\pi$ stacking. Indeed, the V shape of the molecule where the alkyl chains extend outward of the central structure (Figure S31) would allow $\pi\cdots\pi$ stacking to occur with the ethylhexyl chains occupying the voids. As such, coadsorbing agents are still required to improve the cell efficiency. Concerning **6a**, an increase in V_{oc} occurs with a concentration of 10 mM CDCA, leading to an improvement of efficiency from 2.51 to 3.15% and reaching 75% of the standard cell based on dye N-719. This was the best result in this study. No significant differences were observed for compounds **6b** and **6d**.

To understand the discrepancy between the J_{sc} values, the incident photon-to-current efficiency (IPCE) against the wavelength was recorded. IPCE is the product of electron injection efficiency from the dye's excited state (η_{inj}), light-harvesting efficiency (LHE), and charge collection efficiency (η_{coll}) (eq 1):

$$\text{IPCE} = \eta_{inj} \times \text{LHE}(\lambda) \times \eta_{coll} \qquad (1)$$

The IPCE spectra are displayed on Figure 6 and have a good overlap with the absorption spectra of the dyes (Figure S30).
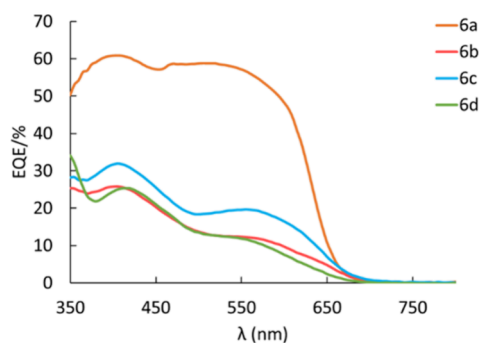
Figure 6. IPCE spectra for the DSSCs based on dyes **6a−d** (best performing cell, [CDCA] = 0 mM).

The dyes showed maximum IPCE values at 400−410 nm, which were 60.8, 25.8, 31.9, and 25.3% for **6a**, **6b**, **6c**, and **6d**, respectively. The IPCE spectrum of **6a** is much higher when compared to those obtained for the other dyes, reaching IPCE values around 60% in wavelength ranges from 400 to 550 nm.

The LHE can be considered 100% for dye-loaded films with thickness over 10 μm.[43] Because the thickness of the anodes used in this work is 15 μm and IPCE is directly correlated with electron injection efficiency (η_{inj}), it may be considered that **6a** has a more efficient electron injection when compared to the other dyes. The fact that the more planar dyes did not show similar performance, even in the presence of CDCA, suggests that electron hole recombination is favored in the more planar dyes and the twisted conformation assumed by the phenyl ring in **6a** reduces the recombination, thus favoring efficient electron injection.[40]

Theoretical Calculations. To explore the geometry and electronic properties of the dyes, theoretical analysis (DFT/CAM-B3LYP/6-311G(d,p) level taking into account the solvent effects of *N*,*N*-dimethylformamide) was performed with Gaussian 09 (Figure 7, Table 4). Frequency analyses for each compound were also computed and did not yield any imaginary frequencies, indicating that the optimized structure of each molecule corresponds to at least a local minimum on the potential energy surface. The time-dependent density functional theory (TD-DFT) approach was used on the previously optimized ground-state molecular geometries to obtain the vertical excitation energies, oscillator strengths (f), dipole moment, and excited-state compositions in terms of excitations between the occupied and virtual orbitals for the investigated compounds (Table 4). Although, for aromatic donor−acceptor systems, it is known that the TD-DFT approach overestimates the absorption wavelengths of CT-type transitions (with errors of up to 1 eV),[44] in our case, the predicted transitions (deviations in the 0.07−0.64 eV range, Tables 1 and 4) and the calculated frontier molecular orbitals band gaps (see Table 2 with the cyclic voltammetry data) are found to be in good agreement to the experimental values
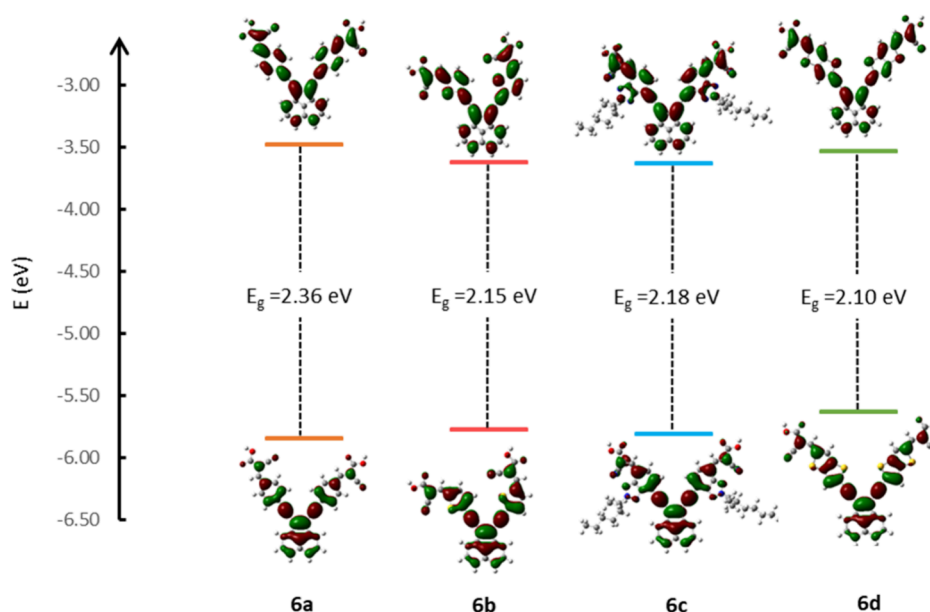
Figure 7. Optimized structures and frontier molecular orbitals (MO) of HOMO and LUMO calculated with DFT on a B3LYP/6-311G(d,p) level of the dyes. The theoretical optical band gaps (E_g's) are also included.

Table 4. Computed Absorption Properties (Predicted Vertical Excitation Energies and Associated Orbital Transition Major Contributions Together with Oscillator Strengths, f, and Dipole Moments) for Chromophores 6a–d Obtained by TD-DFT at the CAM-B3LYP/6-311G(d,p) Level (Using the Polarizable Continuum Model, PCM, to Take into Account the Solvent Effects of N,N-Dimethylformamide) after Ground-State Geometry Optimization Using the Same Functional and Basis Set

dye	λ_{max1} (nm)	λ_{max2} (nm)	dipole moment (debye)	transition and orbital major contributions	oscillator strength, f λ_{max1}	oscillator strength, f λ_{max2}	HOMO (eV)	LUMO (eV)	E_g (eV)
6a	377	501	9.5	$S_0 \rightarrow S_1$, HOMO → LUMO (95%)	0.80	2.61	−5.85	−3.48	2.36
6b	413	548	10.7	$S_0 \rightarrow S_1$, HOMO → LUMO (98%)	0.73	2.15	−5.77	−3.62	2.15
6c	479	685	7.9	$S_0 \rightarrow S_1$, HOMO → LUMO (97%)	1.00	1.63	−5.81	−3.63	2.18
6d	411	591	5.7	$S_0 \rightarrow S_1$, HOMO → LUMO (98%)	0.94	2.81	−5.63	−3.53	2.10

obtained, thus giving additional support for the calculated molecular geometries. In general, the observed lowest energy absorption bands are associated with the predicted $S_0 \rightarrow S_1$ transitions (f values in the 1.6288−2.8073 range) and contributions mainly associated with the HOMO → LUMO orbitals (Table 4). The frontier molecular orbital energy levels and their electron distribution surface plots are shown in Figure 7. For all the compounds, there is an increase in the electronic density in the cyanoacrylic acid moieties upon the transition from HOMO to LUMO. Compound 6a seems to have a slightly more evident intramolecular charge separation than 6b, 6c, and 6d, where a larger overlap between HOMO and LUMO densities is observed. This indicates that the HOMO−LUMO excitation moves the electron distribution from the donor to the acceptor, giving support to an efficient photoinduced charge transfer from the dyes to the CB of the semiconductor, which is more evident in the case of 6a. In the latter compound, a smaller overlap between HOMO and LUMO densities improves the charge separation and is expected to impact both efficiency of the electron injection and the reduction of the charge recombination.

EXPERIMENTAL SECTION (MATERIALS AND METHODS)

Synthesis. The solvents and reagents were purchased from Merck KGaA (Darmstadt, Germany) and used without further purification. Solvent drying was performed by using M2A molecular sieves (Merck KGaA) according to the literature.[45]

Thin-layer chromatography (TLC) was performed on aluminum-backed Kieselgel 60 F254 silica gel plates (Merck KGaA). Plates were visualized with UV light (254 and 336 nm). Preparative-layer chromatography (PLC) was performed on Keiselgel 60 F254 silica gel plates (Merck KGaA). Column chromatography was performed using Kieselgel 60A (Carlo Erba) with particle size 40−63 μm in normal phase.[46]

The ^{1}H and ^{13}C nuclear magnetic resonance (NMR) spectra were recorded in a Bruker Avance III 400 (Billerica, MA, USA) at 400 and 101 MHz, respectively. High-resolution mass spectra (HRMS) were obtained at the University of Salamanca, research support service NUCLEUS, with a Thermo Vanquish core HPLC coupled to a diode array ultraviolet detector and a mass spectrometer (Thermo Orbitrap QExactive Focus).

1,2-Dibromoacenaphthylene (2). The compound 1,2-dibromoacenaphthylene (2) was synthesized according to the literature procedures.[31,32] A solution containing 499.3 mg of acenaphthene (1) (3.24 mmol), 79.1 mg of benzoyl peroxide (0.33 mmol, 0.1 mmol), and 1.7318 g of N-bromosuccinimide (9.73 mmol, 3.00 equiv) in CCl$_4$ was refluxed under a nitrogen

atmosphere for 4 h. The reaction was monitored by TLC using the eluent hexane/EtOAc 9:1. The reaction mixture was filtered to remove the solid. An aqueous solution of Na$_2$S$_2$O$_5$ 1 M was added to the filtrate, and it was extracted with CH$_2$Cl$_2$. The organic phases were washed with water and brine and then dried with anhydrous Na$_2$SO$_4$, filtered, and evaporated. The crude was absorbed in Celite and purified by flash column chromatography using the eluent petroleum ether. It was possible to afford 439.1 mg of a crystalline yellow solid, corresponding to 1,2-dibromoacenaphthylene (2) (η = 44%). ^{1}H NMR (400 MHz, CDCl$_3$) δ (ppm): 7.84 (d, J = 8.4 Hz, 2H), 7.66 (d, J = 6.8 Hz, 2H), 7.57 (t, J = 7.6 Hz, 2H).

1,2-Bis((trimethylsilyl)ethynyl)acenaphthylene (4). To a sealed tube, 345.6 mg of 1,2-dibromoacenaphthylene (2) (1.12 mmol, 1 equiv), Pd(PPh$_3$)$_4$ (0.30 equiv), CuI (0.24 equiv), PPh$_3$ (0.12 equiv), diisopropylamine (3 equiv), and 6 mL of dioxane were added under a N$_2$ atmosphere. The mixture was stirred at 40 °C for 7 h, and then 3 equiv of ethynyltrimethylsilane was added. The consumption of the starting material was monitored by TLC using petroleum ether as the eluent. After 20 h, the reaction was complete, and the solvent was removed under reduced pressure. The crude product was washed with water and extracted with dichloromethane. The combined organic layers were dried over Na$_2$SO$_4$, filtered, and evaporated to dryness. The crude was purified via column chromatography using the eluent CH$_2$Cl$_2$/petroleum ether 9.5:0.5. It was possible to afford an orange oil corresponding to 1,2-bis((trimethylsilyl)ethynyl)-acenaphthylene (4) (229.5 mg, η = 60%). ^{1}H NMR (400 MHz, CDCl$_3$) δ (ppm): 7.86 (d, J = 8.0 Hz, 2H), 7.81 (d, J = 7.2 Hz, 2H), 7.59 (dd, J = 8.2, 7.0 Hz, 2H), 0.34 (s, 18H). ^{13}C NMR (101 MHz, CDCl$_3$) δ (ppm): 138.28, 128.70, 128.31, 128.23, 127.93, 127.31, 124.10, 106.59, 99.31, 0.27. HRMS-ESI(+) calcd for C$_{22}$H$_{24}$Si$_2$ [M + H] 345.14893; found: 345.1486.

7-Bromo-2-(2-ethylhexyl)-2H-benzo[d][1,2,3]triazole-4-carbaldehyde (5c). 2-(2-Ethylhexyl)-2H-benzotriazole. To a round-bottom flask under a N$_2$ atmosphere were added methanol (9 mL), 1,2,3-benzotriazole (0.599 mg, 5.03 mmol, 1 equiv), potassium *tert*-butoxide (848 mg, 7.55 mmol, 1.5 equiv), and bromo-2-ethylhexane (1.04 mL, 5.84 mmol, 1.16 equiv). The reaction mixture was stirred at reflux for 118 h. After cooling, the solvent was removed, and the crude was dissolved in chloroform, washed with water, dried with anhydrous Na$_2$SO$_4$, filtered, and evaporated. The residue was purified by flash column chromatography using the eluent petroleum ether/EtOAc 9:1.[33] It was possible to afford two isomers: 2-(2-ethylhexyl)-2H-benzotriazole (colorless oil) (η =

42%) ^{1}H NMR (400 MHz,CDCl$_3$) δ (ppm): 7.86 (dd, J = 6.6, 3.0 Hz, 2H), 7.37 (dd, J = 6.6, 3.0 Hz, 2H), 4.63 (d, J = 7.2 Hz, 2H), 2.23 (m, 1H), 1.37−1.24 (m, 8H), 0.92 (t, J = 7.6 Hz, 3H, H2), 0.87 (t, J = 7.0 Hz, 3H) and also 2-(2-ethylhexyl)-1H-benzotriazole (η = 38.5%) ^{1}H NMR (400 MHz, CDCl$_3$) δ (ppm): 8.06 (d, J = 8.4 Hz, 1H), 7.49 (m, 2H), 7.35 (ddd, J = 8.0, 6.4, 1.4 Hz, 1H), 4.52 (d, J = 7.2 Hz, 2H), 2.09 (m, 1H), 1.36−1.24 (m, 8H), 0.93 (d, J = 7.4 Hz, 3H), 0.86 (t, J = 7.0 Hz, 3H).

4,7-Dibromo-2-(2-ethylhexyl)benzotriazole. To a round-bottom flask containing 2-(2-ethylhexyl)-2H-benzotriazole (484.8 mg, 2.1 mmol) was added 3.43 mL of and aqueous HBr solution (5.8 M). The reactional mixture was stirred for 1 h at 100 °C. Then 0.35 mL of Br$_2$ (6.64 mmol, 3.2 equiv) was added, and the mixture was stirred for 24 h and 30 min. After cooling to room temperature, the mixture was dissolved in CH$_2$Cl$_2$ and washed with a solution of NaHCO$_3$. The combined organic layers were dried with Na$_2$SO$_4$, filtered, and evaporated. The crude was purified by flash column chromatography (eluent: petroleum ether/CH$_2$Cl$_2$ 6:4). It was possible to afford 481.6 mg of a yellow oil corresponding to 4,7-dibromo-2-(2-ethylhexyl)benzotriazole (η = 59%). ^{1}H NMR (400 MHz, CDCl$_3$) δ(ppm): 7.44 (s, 2H), 4.68 (d, J = 7.2 Hz, 2H), 2.30 (m, 1H), 1.33 (m, 8H), 0.92 (t, J = 7.6 Hz, 3H), 0.87 (t, J = 6.8 Hz, 3H).[33]

7-Bromo-2-(2-ethylhexyl)-2H-benzo[d][1,2,3]triazole-4-carbaldehyde (5c). To a round-bottom flask containing 257 mg of 4,7-dibromo-2-(2-ethylhexyl)benzotriazole (0.66 mmol) was added 3.8 mL of dry THF, and the mixture was cooled to −78 °C in an acetone/liquid N$_2$ bath. Then 0.62 mL of a 1.17 M solution of n-BuLi in hexanes (0.73 mmol, 1.1 equiv) was added dropwise. After 15 min, 51 μL of dry DMF (1 equiv) was added, and the reaction was stirred for more 3 h at −78 °C. The consumption of the starting material was confirmed by TLC using the eluent petroleum ether/EtOAc 9:1. Then the reaction was warmed to room temperature, and H$_2$O was added. The organic product was extracted with CH$_2$Cl$_2$. The combined organic layers were dried over Na$_2$SO$_4$, filtered, and evaporated. The resulting crude was subjected to flash column chromatography (eluent: petroleum ether/EtOAc 9:1) to afford 139.4 mg of a colorless oil corresponding to 7-bromo-2-(2-ethylhexyl)-2H-benzo[d][1,2,3]triazole-4-carbaldehyde (5c) (0.41 mmol, η = 62%). ^{1}H NMR (400 MHz, CDCl$_3$) δ (ppm): 10.47 (s, 1H), 7.83 (d, J = 7.6 Hz, 1H), 7.75 (d, J = 7.6 Hz, 1H), 4.74 (d, J = 7.3 Hz, 2H), 2.39−2.28 (m, 1H), 1.40−1.23 (m, 9H), 0.93 (t, J = 7.6 Hz, 3H), 0.87 (t, J = 7.0 Hz, 3H). ^{13}C NMR (101 MHz, CDCl$_3$) δ (ppm): 188.99, 144.95, 141.70, 131.15, 128.83, 125.72, 118.99, 61.05, 40.47, 30.43, 28.40, 23.88, 22.98, 14.08, 10.49. HRMS-ESI(+) calcd for C$_{15}$H$_{20}$BrN$_3$O [M + H] 338.08625; found: 338.0856

5-Bromothieno-[3,2-b]-tiophene-2-carbaldehyde (5d). Starting from 150 mg of 2,5-dibromothieno-[3,2-b]thiophene (0.50 mmol) it was followed the same procedure as for 5c. The crude was purified by flash chromatography column using the eluent petroleum ether/CH$_2$Cl$_2$ 8:2, and 70 mg of a white/yellow solid was obtained corresponding to 5-bromothieno-[3,2-b]-thiophene-2-carbaldehyde (5d) (0.28 mmol, η = 57%). ^{1}H NMR (400 MHz, CDCl$_3$) δ (ppm): 9.97 (s, 1H), 7.84 (s, 1H), 7.36 (s, 1H).[29]

Compound 3a. 1,2-Dibromoacenaphthylene (2) (50.17 mg, mmol, 0.16 mmol), PPh$_3$ (5.33 mg, 0.02 mmol, 0.12 equiv), CuI (7.76 mg, 0.04 mmol, 0.25 equiv), 4-ethynylbenzaldehyde (63.56 mg, 0.49 mmol, 3.05 equiv),

and Pd(PPh$_3$)$_4$ (59.3 mg, 0.05 mmol, 0.32 equiv) were added to a Schlenk tube under a N$_2$ atmosphere. Then 4 mL of dry dioxane and 68 μL of diisopropylamine (0.49 mmol, 3.03 equiv) were added, and the reaction mixture was degassed under a vacuum. The reaction mixture was stirred for 19 h and 30 min at 60 °C; it was followed by TLC using the eluent hexane/EtOAc 7:3. The solvent was removed, H$_2$O was added, and the organic product was extracted with CH$_2$Cl$_2$. The combined organic layers were dried over Na$_2$SO$_4$, filtered, and evaporated to dryness. The crude was purified via column chromatography using CH$_2$Cl$_2$ as eluent to afford 49.9 mg of a red solid corresponding to 4,4′-(acenaphthylene-1,2-diylbis-(ethyne-2,1-diyl))dibenzaldehyde (3a) (η = 76%). ^{1}H NMR (400 MHz, CDCl$_3$) δ (ppm): 10.06 (s, 2H), 7.95 (m, 8H), 7.82 (d, J = 7.6 Hz, 4H), 7.69 (t, J = 7.6 Hz, 2H). ^{13}C NMR (126 MHz, DMSO) δ (ppm): 192.06, 136.77, 135.84, 131.21, 129.55, 128.68, 128.51, 127.92, 127.60, 126.49, 125.83, 124.62, 100.04, 87.34. HRMS-ESI(+) calcd for C$_{30}$H$_{16}$O$_2$ [M + H] 409.12231; found: 409.1216.

Synthesis of Aldehydes (3b−d). To a solution of 1,2-bis((trimethylsilyl)ethynyl)acenaphthylene (4) (1 equiv) in methanol and dioxane (1:1) was added K$_2$CO$_3$ (2 equiv). The reaction was monitored by TLC using the eluent petroleum ether/EtOAc 6:4. After the consumption of the starting material, the reactional mixture containing 1,2-diethynylace-naphthylene was directly transferred to the next reactional step. In a Schlenk tube were added under a N$_2$ atmosphere bromoaldehyde (2.2 equiv), (PdPPh$_3$)$_4$ (0.20 equiv), CuI (0.24 equiv), PPh$_3$ (0.12 equiv), diisopropylamine (3 equiv), and 4 mL of dioxane. The reaction was degassed, and then it was stirred for 3 h at 40 °C. Then the reactional mixture containing 1,2-diethynylacenaphthylene (1 equiv) was added, and the solution was degassed again under a vacuum. The reaction was monitored by TLC. After consumption of the starting material, the solvent was removed, water was added, and the organic compound was extracted with dichloro-methane. The combined organic layers were dried over anhydrous Na$_2$SO$_4$, filtered, and evaporated to dryness. The crude was purified via column chromatography

Compound 3b. Compound 3b was prepared following the general procedure starting from 5-bromothiophene-2-carbalde-hyde (0.37 mmol, 2.2 equiv) and 1,2 bis((trimethylsilyl)-ethynyl)acenaphthylene (0.17 mmol, 1 equiv). The reaction was monitored by TLC using the eluent petroleum ether/EtOAc 6:4, and after 24 h, the reaction was complete. The crude was purified via column chromatography using as eluent CH$_2$Cl$_2$/petroleum ether 9.5:0.5, and then one of the collected fractions was subjected to preparative layer plate chromatog-raphy (PLC) to afford 44.2 mg of a red solid corresponding to 5,5′-(acenaphthylene-1,2-diylbis(ethyne-2,1-diyl))bis-(thiophene-2-carbaldehyde) (3b) (η = 62%). ^{1}H NMR (400 MHz, CDCl$_3$) δ (ppm): 9.91 (s, 2H), 7.94 (d, J = 8.0 Hz, 2H), 7.90 (d, J = 6.8 Hz, 2H), 7.72 (d, J = 4.0 Hz, 2H), 7.66 (t, 2H), 7.44 (d, J = 4.0 Hz, 2H). ^{13}C NMR (101 MHz, CDCl$_3$) δ (ppm): 182.47, 144.73, 137.56, 136.26, 133.29, 132.45, 129.56, 128.63, 128.55, 127.73, 126.83, 124.73, 93.71, 93.23. HRMS-ESI(+) calcd for C$_{26}$H$_{12}$O$_2$^{32}S$_2$ [M + H] 421.03515; found: 421.0344.

Compound 3c. Compound 3c was prepared following the general procedure starting from 7-bromo-2-(2-ethylhexyl)-2H-benzo[d][1,2,3]triazole-4-carbaldehyde (5c) (0.38 mmol, 2.2 equiv) and 1,2-bis((trimethylsilyl)ethynyl)acenaphthylene (0.17 mmol, 1 equiv). The reaction was monitored by TLC

using the eluent petroleum ether/EtOAc 8:2, and after 21 h and 30 min, the reaction was complete. The crude was purified via column chromatography using CH_2Cl_2 as the eluent. One of the collected fractions was subjected to preparative layer plate chromatography (PLC) using a mixture of CH_2Cl_2 with 0.5% of MeOH to afford 67.7 mg of a dark red solid corresponding to 7,7′-(acenaphthylene-1,2-diylbis(ethyne-2,1-diyl))bis(2-(2-ethylhexyl)-2H-benzo[d][1,2,3]triazole-4-carbaldehyde) (**3c**) (0.095 mmol, η = 54%). ^{1}H NMR (400 MHz, CDCl$_3$) δ (ppm): 10.52 (s, 2H), 8.12 (d, J = 6.9 Hz, 2H), 7.98 (d, J = 8.5 Hz, 4H), 7.87 (d, J = 7.4 Hz, 2H), 7.74−7.68 (m, 2H), 4.78 (d, J = 7.1 Hz, 4H), 2.36 (dt, J = 12.3, 6.3 Hz, 2H), 1.44−1.24 (m, 19H), 0.95 (t, J = 7.4 Hz, 6H), 0.86 (t, J = 7.0 Hz, 6H). ^{13}C NMR (101 MHz, CDCl$_3$) δ (ppm): 189.01, 145.51, 141.86, 138.26, 130.06, 129.55, 129.44, 128.64, 128.49, 127.99, 127.35, 126.08, 124.97, 120.42, 97.10, 9.10, 60.68, 40.50, 30.54, 28.49, 23.94, 22.99, 14.11, 10.54. HRMS-ESI(+) calcd for $C_{46}H_{46}N_6O_2$ [M + H] 715.37549; found 715.3748.

Compound 3d. Compound **3d** was prepared following the general procedure starting from 5-bromothieno-[3,2-b]-tiophene-2-carbaldehyde (**5d**) (0.28 mmol, 2.2 equiv) and 1,2 bis((trimethylsilyl)ethynyl)acenaphthylene (0.13 mmol, 1 equiv). The reaction was monitored by TLC using the eluent petroleum ether/EtOAc 8:2, and after 20 h, the consumption of the starting material was observed. The crude was purified by column chromatography using the eluent CH_2Cl_2/petroleum ether to CH_2Cl_2/MeOH 5%. The fraction containing the product was washed with ethanol to remove some of the impurities. A dark red solid (37.3 mg) was obtained corresponding to 5,5′-(acenaphthylene-1,2-diylbis-(ethyne-2,1-diyl))bis(thieno[3,2-b]thiophene-2-carbaldehyde) (**3d**) (0.07 mmol, η = 54%). ^{1}H NMR (400 MHz,CDCl$_3$) δ (ppm): 10.01 (s, 2H), 7.99−7.92 (m, 6H), 7.72−7.67 (m, 3H), 7.63 (s, 2H). HRMS-ESI(+) calcd for $C_{30}H_{12}O_2S_4$ [M + Na] 554.96123; found: 554.9603.

Compound 6a. A mixture of 4,4′-(acenaphthylene-1,2-diylbis(ethyne-2,1-diyl))dibenzaldehyde (**3a**) (25.1 mg, 0.061 mmol), cyanoacetic acid (33.5 mg, 0.39 mmol, 6.5 equiv), 34 μL of piperidine (0.34 mmol, 5.6 equiv), and 3 mL of acetonitrile was refluxed under a N_2 atmosphere for 16 h. The consumption of the start material was monitored by TLC using the eluent hexane/EtOAc 6:4. The solvent was removed under reduced pressure, and the crude product was washed with hexane to remove nonpolar impurities. The resulting solid was dissolved in methanol, and 1 M HCl was added. The mixture was taken to dryness, and the solid was washed with H_2O to remove salts and then with ethanol. It was obtained as a dark red/purple solid corresponding to 3,3′-((acenaphthylene-1,2-diylbis(ethyne-2,1-diyl))bis(4,1-phenylene))bis(2-cyanoacrylic acid) (**6a**) (23.4 mg, η = 70%). ^{1}H NMR (400 MHz, DMSO) δ (ppm): 8.39 (s, 2H), 8.15 (m, 8H), 7.95 (d, J = 8.4 Hz, 4H), 7.81 (t, J = 7.4 Hz, 2H). HRMS-ESI(−) calcd for $C_{36}H_{18}O_4N_2$ [M-H] 541.11938; found: 541.1202.

Compound 6b. Following the same procedure for **6a** and starting from 31,7 mg of 5,5′-(acenaphthylene-1,2-diylbis-(ethyne-2,1-diyl))bis(thiophene-2-carbaldehyde) (**3b**) (0.075 mmol), the reaction was monitored by TLC using the eluent CH_2Cl_2. The solvent was removed under reduced pressure, and the solid was washed with acetonitrile. Then the resulting solid was dissolved in a mixture of CH_2Cl_2/MeOH/H_2O (65/35/5, % v/v), and 1 M HCl was added. The mixture was taken to dryness, and the solid was washed with H_2O to remove salts. To remove the less polar impurities, the solid was washed with hexane, ethyl acetate, and ethanol. It was possible to obtain a dark red/brown solid corresponding to 3,3′-((acenaphthylene-1,2-diylbis(ethyne-2,1-diyl))bis(thiophene-5,2-diyl))bis(2-cyanoacrylic acid) (**6b**) (20.7 mg, η = 50%). ^{1}H NMR (400 MHz, DMSO-d6) δ (ppm): 8.54 (s, 2H), 8.17 (d, J = 8.3 Hz, 2H), 8.10 (d, J = 8.0 Hz, 2H), 8.05 (d, J = 4.1 Hz, 2H), 7.80 (t, J = 7.8 Hz, 4H), 7.75 (d, J = 3.9 Hz, 2H). HRMS-ESI(−) calcd for $C_{32}H_{14}N_2O_4S_2$ [M-H] 553.03222; found: 553.0326.

Compound 6c. Following the procedure for compound **6a** and starting with 7,7′-(acenaphthylene-1,2-diylbis(ethyne-2,1-diyl))bis(2-(2-ethylhexyl)-2H-benzo[d][1,2,3]triazole-4-carbaldehyde) (**3c**) (40.1 mg, 0.063 mmol, 1 equiv), the reaction was followed by TLC using the eluents CH_2Cl_2/MeOH/H_2O (65/10/1, % v/v) and petroleum ether/EtOAc 8:2, and after 25 h, the reaction was complete. The solvent was removed, and the solid was washed with acetonitrile. Then the resulting solid was dissolved in a mixture of CH_2Cl_2/MeOH/H_2O (65/35/5, % v/v), and 1 M HCl was added. The mixture was taken to dryness, and the solid was washed with H_2O to remove salts to afford 3,3′-((acenaphthylene-1,2-diylbis(ethyne-2,1-diyl))bis-(2-(2-ethylhexyl)-2H-benzo[d][1,2,3]triazole-7,4-diyl))bis(2-cyanoacrylic acid) (**6c**) (44.2 mg, 0.052 mmol, η = 83%). ^{1}H NMR (400 MHz, DMSO-d_6) δ (ppm): 8.44 (s, 2H, CH$_2$), 8.13 (d, J = 7.6 Hz, 2H), 7.87 (d, J = 8.2 Hz, 2H), 7.74 (d, J = 6.6 Hz, 2H), 7.65 (d, J = 7.4 Hz, 2H), 7.52 (t, J = 7.3 Hz, 2H), 4.57 (d, J = 6.0 Hz, 4H), 2.10−1.98 (m, 2H), 1.18 (m, 7.7 Hz, 19H), 0.79 (t, J = 7.4 Hz, 6H), 0.75−0.68 (m, 7H). HRMS-ESI(−) calcd for $C_{52}H_{48}N_8O_4$ [M-H] 847.37257; found: 847.3726.

Compound 6d. Following the procedure for compound **6a** and starting with 5,5′-(acenaphthylene-1,2-diylbis(ethyne-2,1-diyl))bis(thieno[3,2-b]thiophene-2-carbaldehyde) (**3d**) (35.3 mg, 0.066 mmol, 1 equiv), the reaction was first stirred at room temperature and after 40 h was warmed to 80 °C, and then it was stirred for 33 h more. The reaction was monitored by TLC using the eluents CH_2Cl_2/MeOH/H_2O (65/10/1, % v/v and petroleum ether/EtOAc 8:2. When it was completed, the solvent was removed, the solid was dissolved in a mixture of CH_2Cl_2/MeOH/H_2O (65/35/5, % v/v), and 1 M HCl was added. The mixture was taken to dryness, and the solid was washed with H_2O to remove salts and then with acetonitrile and CH_2Cl_2 to afford 33 mg of 3,3′-((acenaphthylene-1,2-diylbis(ethyne-2,1-diyl))bis(thieno[3,2-b]thiophene-5,2-diyl))-bis(2-cyanoacrylic acid) (**6d**) (0.049 mmol, η = 75%). ^{1}H NMR (400 MHz, DMSO-d_6) δ (ppm): 8.52 (s, 2H), 8.26 (s, 2H), 8.16−7.96 (m, 6H), 7.82−7.70 (m, 2H). HRMS-ESI(−) calculated for: $C_{36}H_{14}N_2O_4S_4$ [M-H] 664.97636; found: 664.9767.

Characterization. *Spectroscopic Characterization.* Absorption spectra were recorded on a VWR M4 spectrometer (Ismaning, Germany). Fluorescence spectra were acquired on a SPEX Fluorolog 1681 0.22 m spectrofluorimeter (Metuchen, NJ, USA) equipped with a 150 W Xe−Hg lamp, which were then corrected for the system's wavelength response.

Electrochemical Characterization. Cyclic voltammetry (CV) measurements were carried out on an μAutolab Type III potentiostat/galvanostat (Metrohm Autolab B.V., Utrecht, The Netherlands) monitored by the GPES (General Purpose Electrochemical System) software, version 4.9 (Eco-Chemie, B.V. Software, Utrecht, The Netherlands). The three-electrode cell used was cylindrical and had a capacity of 5 mL. A saturated calomel electrode (SCE, saturated KCl) reference electrode (Metrohm, Utrecht, The Netherlands) was used as

the standard for all of the measurements. A glassy carbon electrode (MF-2013, f = 1.6 mm, BAS Inc.,West Lafayette, IN, USA) was employed as the working electrode and a Pt wire as the counter electrode. Before use, the working electrode was polished using 1.0 and 0.3 mm alumina aqueous suspensions (Buehler, Esslingen, Germany) over 2−7/" microcloth (Buehler) polishing pads and then rinsed with water and ethanol. Before any electrochemical measurements were performed, this cleaning technique was constantly applied. The electrolyte contained a solution of 0.1 M tetrabutylammonium hexafluorophosphate (TBAPF$_6$) in dry DMF, with a dye concentration of 1.5×10^{-4} M. Measurements were performed with a scan rate of 50, 100, 250, and 500 mV s^{-1}. Before and throughout the electrochemical measurements, the solutions were deaerated by purging with N$_2$. The onset values were considered the crossing points between the tangent lines of the rising current and the baseline current.

DSSC Fabrication and Photovoltaic Characterization. The detailed procedure has been described elsewhere.[47] The conductive FTO-glass (TEC7, Greatcell Solar) used to make the transparent electrodes was initially cleaned with soap and then washed with water and ethanol. To prepare the anodes, the FTO-glass plates were coated with a TiCl$_4$/water solution (40 mM) at 70 °C for 30 min, after which they were rinsed with water and ethanol and sintered at 500 °C for 30 min. This procedure functions as a "blocking layer", preventing charge recombination between electrons in the FTO, and it also enhances the adherence of the subsequently deposited nanocrystalline layers to the glass plates. Later, by using a 43.80 mesh per cm^2 polyester fiber frame and using a titania paste (18NR-T, Greatcell Solar, Queanbeyan, Australia), the transparent TiO$_2$ layers were deposited on the already prepared plates through the screen-printing technique. The plates containing the deposited films were heated to 125 °C on a heating plate to dry them, and then, the coating and drying process was performed once more. The temperature of the TiO$_2$-coated plates was progressively raised to 325 °C, then to 375 °C in 5 min, and lastly to 500 °C. The plates were sintered for 30 min at this temperature and then cooled down to room temperature. Following the aforementioned protocol, the treatment with TiCl$_4$/water solution (40 mM) was repeated. The screen-printing deposition of reflective titania paste (WER2-O, Greatcell Solar) and sinterization at 500 °C completed the anode fabrication. This layer of 150−200 nm sized anatase particles helps enhance the photocurrent. The plates containing the anodes were divided into rectangles (size: 2 × 1.5 cm) containing a spot area of 0.196 cm^2 with a thickness of 15 μm. The anodes were immersed for 16 h in a 0.5 mM solution of the dye in CH$_2$Cl$_2$/MeOH/H$_2$O (65:35:5, % v/v) at room temperature protected from the light. The photoanodes were rinsed with the same solvent to remove the excess dye.

The cathodes were made of a 2 × 2 cm FTO-glass plate in which a hole (1.0 mm diameter) was drilled. To get rid of any remaining glass powder and organic contaminants, the glass plates were then washed and cleaned with water and ethanol. The transparent Pt catalyst (PT1, Greatcell Solar) was deposited on the conductive face of the FTO-glass by a doctor blade technique. A strip of adhesive tape (3M Magic) was placed along 0.5 cm of the edge of the glass to control the thickness of the deposited layer and to mask an electrical contact strip. The Pt paste was uniformly distributed across the substrate by sliding a glass rod along the tape spacer. The

adhesive tape strip was taken off, and the cathodes were heated for 30 min at 550 °C. By use of a thermopress, the photoanode and the cathode were assembled into a sandwich-type configuration. A Surlyn ionomer (Meltonix 1170-25, Solaronix SA) was used to seal the cells. The redox couple I$^-$/I$_3^-$ (0.8 M LiI and 0.05 M I$_2$) was dissolved in a mixture of acetonitrile/valeronitrile (85:15, % v/v) to prepare the electrolyte employed in this work. The electrolyte introduction into the cell was done by filling under a vacuum through the hole drilled in the cathode followed by sealing with adhesive tape. For each compound, at least two cells were assembled under the same conditions, and the efficiencies were measured five times for each cell.

Photoelectrochemical Measurements. Photocurrent voltage measurements were performed using a Keithley SourceMeter multimeter, and an Oriel solar simulator (Model LCS-100 Small Area Sol1A, 300 W Xe Arc lamp equipped with AM 1.5 G filter, 100 mW cm^{-2}) was used to simulate sunlight irradiation. The incident photon to current conversion efficiency (IPCE) of the photovoltaic devices was measured as a function of wavelength from 350 to 800 nm, and it was performed in a Newport QuantX-300 system containing a 100 W Xe lamp (Montana, USA).

Computational Details. The calculations were performed by using Gaussian 09. The geometries of the dyes were optimized by DFT calculations using the B3LYP/6-311G(d,p) method.[48,49] The molecular structures were optimized without conformation restrictions, and the frequency analyses were performed at the same level of theory as geometry optimizations to confirm that all optimized structures are a local minimum on the potential energy surface. Time-dependent density functional theory (TD-DFT)[50,51] calculations at the B3LYP/6-311g(d,p) level were used on the previously optimized ground-state molecular geometries to obtain vertical excitation energies, oscillator strengths (f), dipole moments, and active molecular orbitals with their highest contribution percentage. The polarizable continuum model (PCM) was employed to account for the solvation effects of *N*,*N*-dimethylformamide, which was used in the spectroscopic and electrochemical characterization. The molecular orbital contours were plotted using the GaussView 5.0 program.

■ CONCLUSIONS

Four diethynylacenaphthylene dyes with different aryl π-bridges were synthesized and tested as sensitizers for dye-sensitized solar cells (DSSCs). Extension of the conjugated system involved Sonogashira coupling reactions with reasonable yields. Spectroscopic characterization of the systems shows that all compounds are red-shifted relative to the parent phenyl-bridged derivative, in accordance with TD-DFT calculations. Spectroscopic and electrochemical data allowed to prove that the HOMO and LUMO energies of the four dyes are adequately located above the CB of TiO$_2$ and below the I$^-$/I$_3^-$ redox potential, respectively. The overall conversion efficiency of the phenylethynyl derivative **6a** proved to be significantly superior (3- to 7-fold) to the other aryl derivatives **6b−d**, with **6a** showing a 2.51% efficiency that was increased to 3.15% in the presence of CDCA (10 mM). Meanwhile, the molecular design of the acenaphthylene dyes, with two arylethynyl π-bridges (dianchoring dyes) here described, paves the way for the development of novel acenaphthylene-based dyes for DSSC applications with improved efficiency.

ASSOCIATED CONTENT

Data Availability Statement

The data underlying this study are available in the published article and in its Supporting Information.

Supporting Information

The Supporting Information is available free of charge at https://pubs.acs.org/doi/10.1021/acsomega.4c01201.

General procedures, experimental details, characterization data, NMR spectra (PDF)

AUTHOR INFORMATION

Corresponding Authors

A. Jorge Parola − *LAQV@REQUIMTE, Chemistry Department of Nova School of Science and Technology, Nova University of Lisbon, Caparica 2829-516, Portugal;* orcid.org/0000-0002-1333-9076; Email: paula.branco@campus.fct.unl.pt

Paula S. Branco − *LAQV@REQUIMTE, Chemistry Department of Nova School of Science and Technology, Nova University of Lisbon, Caparica 2829-516, Portugal;* orcid.org/0000-0002-7312-8596; Email: ajp@fct.unl.pt

Authors

Gabriela Malta − *LAQV@REQUIMTE, Chemistry Department of Nova School of Science and Technology, Nova University of Lisbon, Caparica 2829-516, Portugal*

João Pina − *CQC-IMS, Department of Chemistry, University of Coimbra, Coimbra 3004-535, Portugal;* orcid.org/0000-0003-1848-1167

J. Carlos Lima − *LAQV@REQUIMTE, Chemistry Department of Nova School of Science and Technology, Nova University of Lisbon, Caparica 2829-516, Portugal;* orcid.org/0000-0003-0528-1967

Complete contact information is available at:
https://pubs.acs.org/10.1021/acsomega.4c01201

Author Contributions

The contributions of the authors to this work are as follows: conceptualization, P.S.B. and A.J.P.; methodology, P.S.B., A.J.P., J.C.L; laboratory work, G.M.; computational studies, G.M. and J.P.; writing − original draft preparation, P.S.B., A.J.P., and G.M.; writing − review and editing, P.S.B., A.J.P., and J.C.L. All authors have read and agreed to the published version of the manuscript.

Notes

The authors declare no competing financial interest.

ACKNOWLEDGMENTS

REFERENCES

(1) Sanchez, A.; Zhang, Q.; Martin, M.; Vega, P. Towards a New Renewable Power System Using Energy Storage: An Economic and Social Analysis. *Energy Conv. Manag.* **2022**, *252*, No. 115056.

(2) Wang, F.; Harindintwali, J. D.; Yuan, Z.; Wang, M.; Wang, F.; Li, S.; Yin, Z.; Huang, L.; Fu, Y.; Li, L.; Chang, S. X.; Zhang, L.; Rinklebe, J.; Yuan, Z.; Zhu, Q.; Xiang, L.; Tsang, D. C. W.; Xu, L.; Jiang, X.; Liu, J.; Wei, N.; Kästner, M.; Zou, Y.; Ok, Y. S.; Shen, J.; Peng, D.; Zhang, W.; Barceló, D.; Zhou, Y.; Bai, Z.; Li, B.; Zhang, B.; Wei, K.; Cao, H.; Tan, Z.; Zhao, L. b.; He, X.; Zheng, J.; Bolan, N.; Liu, X.; Huang, C.; Dietmann, S.; Luo, M.; Sun, N.; Gong, J.; Gong, Y.; Brahushi, F.; Zhang, T.; Xiao, C.; Li, X.; Chen, W.; Jiao, N.; Lehmann, J.; Zhu, Y. G.; Jin, H.; Schäffer, A.; Tiedje, J. M.; Chen, J. M. Technologies and Perspectives for Achieving Carbon Neutrality. *Innovation* **2021**, *2*, No. 100180.

(3) Dhonde, M.; Sahu, K.; Das, M.; Yadav, A.; Ghosh, P.; Murty, V. V. S. Review-Recent Advancements in Dye-Sensitized Solar Cells; from Photoelectrode to Counter Electrode. *J. Electrochem. Soc.* **2022**, *169*, No. 066507.

(4) Grifoni; Bonomo, M.; Naim, W.; Barbero, N.; Alnasser, T.; Dzeba, I.; Giordano, M.; Tsaturyan, A.; Urbani, M.; Torres, T.; Barolo, C. Toward Sustainable, Colorless, and Transparent Photovoltaics: State of the Art and Perspectives for the Development of Selective near-Infrared Dye-Sensitized Solar Cells. *Adv. Energy Mater.* **2021**, *11*, 2101598.

(5) O'Regan, B.; Grätzel, M. A Low-Cost, High-Efficiency Solar-Cell Based on Dye-Sensitized Colloidal Tio2 Films. *Nature* **1991**, *353*, 737−740.

(6) Schoden, F.; Schnatmann, A. K.; Blachowicz, T.; Manz-Schumacher, H.; Schwenzfeier-Hellkamp, E. Circular Design Principles Applied on Dye-Sensitized Solar Cells. *Sustainability* **2022**, *14*, 15280.

(7) Tao, M.; Hamada, H.; Druffel, T.; Lee, J. J.; Rajeshwar, K. Review-Research Needs for Photovoltaics in the 21st Century. *ECS J. Solid State Sci. Technol.* **2020**, *9*, 125010.

(8) Murakami, T. N.; Koumura, N. Development of Next-Generation Organic-Based Solar Cells: Studies on Dye-Sensitized and Perovskite Solar Cells. *Adv. Energy Mater.* **2019**, *9*, 1802967.

(9) Yahya, M.; Bouziani, A.; Ocak, C.; Seferoglu, Z.; Sillanpaa, M. Organic/Metal-Organic Photosensitizers for Dye-Sensitized Solar Cells (Dssc): Recent Developments, New Trends, and Future Perceptions. *Dyes Pigment.* **2021**, *192*, No. 109227.

(10) Pecnikaj, I.; Minudri, D.; Otero, L.; Fungo, F.; Cavazzini, M.; Orlandi, S.; Pozzi, G. J. Fluorous Molecules for Dye-Sensitized Solar Cells: Synthesis and Properties of Di-Branched, Di-Anchoring Organic Sensitizers Containing Fluorene Subunits. *New J. Chem.* **2017**, *41*, 7729−7738.

(11) Manfredi, N.; Cecconi, B.; Abbotto, A. Multi-Branched Multi-Anchoring Metal-Free Dyes for Dye-Sensitized Solar Cells. *Eur. J. Org. Chem.* **2014**, *2014*, 7069−7086.

(12) Abbotto, A.; Manfredi, N.; Marinzi, C.; De Angelis, F.; Mosconi, E.; Yum, J.-H.; Xianxi, Z.; Nazeeruddin, M. K.; Grätzel, M. Di-Branched Di-Anchoring Organic Dyes for Dye-Sensitized Solar Cells. *Energy Environ. Sci.* **2009**, *2*, 1094−1101.

(13) Sirohi, R.; Kim, D. H.; Yu, S.-C.; Lee, S. H. J. D. Pigments, Novel Di-Anchoring Dye for Dssc by Bridging of Two Mono Anchoring Dye Molecules: A Conformational Approach to Reduce Aggregation. *Dyes Pigments* **2012**, *92*, 1132−1137.

(14) Islam, K.; Narjinari, H.; Kumar, A. Polycyclic Aromatic Hydrocarbons Bearing Polyethynyl Bridges: Synthesis, Photophysical

Properties, and Their Applications. *Asian J. Org. Chem.* **2021**, *10*, 1544−1566.

(15) Jeong, S.; Kim, S. H.; Kim, D. Y.; Kim, C.; Lee, H. W.; Lee, S. E.; Kim, Y. K.; Yoon, S. S. Blue Organic Light-Emitting Diodes Based on Diphenylamino Dibenzo GP Chrysene Derivatives. *Thin Solid Films* **2017**, *636*, 8−14.

(16) Pedersen, S. K.; Pedersen, V. B. R.; Kamounah, F. S.; Brøløs, L. M.; Baryshnikov, G. V.; Valiev, R. R.; Ivaniuk, K.; Stakhira, P.; Minaev, B.; Karaush-Karmazin, N.; Ågren, H.; Pittelkow, M. Dianthracenylazatrioxa 8 Circulene: Synthesis, Characterization and Application in OLEDS. *Chem. - Eur. J.* **2021**, *27*, 11609−11617.

(17) Liu, Y.-H.; Perepichka, D. F. Acenaphthylene as a Building Block for Π-Electron Functional Materials. *J. Mater. Chem. C* **2021**, *9*, 12448−12461.

(18) Reeta, P. S.; Giribabu, L.; Senthilarasu, S.; Hsu, M. H.; Kumar, D. K.; Upadhyaya, H. M.; Robertson, N.; Hewat, T. Ethynyl Thiophene-Appended Unsymmetrical Zinc Porphyrin Sensitizers for Dye-Sensitized Solar Cells. *RSC Adv.* **2014**, *4*, 14165−14175.

(19) Zhang, H.; Chen, Z. E.; Tian, H. R. Molecular Engineering of Metal-Free Organic Sensitizers with Polycyclic Benzenoid Hydrocarbon Donor for Dssc Applications: The Effect of the Conjugate Mode. *Sol. Energy* **2020**, *198*, 239−246.

(20) Wang, T. H.; Han, J. L.; Zhang, Z. Y.; Xu, B.; Huang, J. H.; Su, J. H. Bistriphenylamine-Substituted Fluoranthene Derivatives as Electroluminescent Emitters and Dye-Sensitized Solar Cells. *Tetrahedron* **2012**, *68*, 10372−10377.

(21) Kong, Z. X.; Zhou, H. Z.; Cui, J. N.; Ma, T. L.; Yang, X. C.; Sun, L. C. A New Class of Organic Dyes Based on Acenaphthopyrazine for Dye-Sensitized Solar Cells. *J. Photochem. Photobiol. A-Chem.* **2010**, *213*, 152−157.

(22) Okujima, T.; Shida, Y.; Ohara, K.; Tomimori, Y.; Nishioka, M.; Mori, S.; Nakae, T.; Uno, H. Synthesis of Nir-Emitting O-Chelated Bodipys Fused with Benzene and Acenaphthylene. *J. Porphyr. Phthalocyanines* **2014**, *18*, 752−761.

(23) Xie, Y.; Han, L.; Ge, C.-S.; Cui, Y.-H.; Gao, J.-R. J. C. C. L. Novel Organic Dye Sensitizers Containing Fluorenyl and Biphenyl Moieties for Solar Cells. *Chin. Chem. Lett.* **2017**, *28*, 285−292.

(24) Ji, J. M.; Zhou, H. R.; Eom, Y. K.; Kim, C. H.; Kim, H. K. 14.2% Efficiency Dye-Sensitized Solar Cells by Co-Sensitizing Novel Thieno 3,2-B Indole-Based Organic Dyes with a Promising Porphyrin Sensitizer. *Adv. Energy Mater.* **2020**, *10*, 2000124.

(25) Chen, C.; Hsu, Y.; Chou, H.; Thomas, K. R. J.; Lin, J. T.; Hsu, C. Dipolar Compounds Containing Fluorene and a Heteroaromatic Ring as the Conjugating Bridge for High-Performance Dye-Sensitized Solar Cells. *Chem. - Eur. J.* **2010**, *16*, 3184−3193.

(26) Baheti, A.; Tyagi, P.; Thomas, K. R. J.; Hsu, Y.-C.; Lin, J. T. Simple Triarylamine-Based Dyes Containing Fluorene and Biphenyl Linkers for Efficient Dye-Sensitized Solar Cells. *J. Phys. Chem. C* **2009**, *113*, 8541−8547.

(27) Khanmohammadi Chenab, K.; Zamani Meymian, M. R. Replacing Naphthalene with Anthracene Pi-Bridge Improves Efficiency of D-Pi-a Triphenylamine Dyes-Based Dye-Sensitized Solar Cells. *Solar Energy* **2022**, *234*, 9−20.

(28) Chen, C. C.; Nguyen, V. S.; Chiu, H. C.; Chen, Y. D.; Wei, T. C.; Yeh, C. Y. Anthracene-Bridged Sensitizers for Dye-Sensitized Solar Cells with 37% Efficiency under Dim Light. *Adv. Energy Mater.* **2022**, *12*, 2104051.

(29) Sarrato, J.; Pinto, A. L.; Malta, G.; Rock, E. H.; Pina, J.; Lima, J. C.; Parola, A. J.; Branco, P. S. New 3-Ethynylaryl Coumarin-Based Dyes for Dssc Applications: Synthesis, Spectroscopic Properties, and Theoretical Calculations. *Molecules* **2021**, *26*, 2934.

(30) Zhang, L.; Cole, J. M. Anchoring Groups for Dye-Sensitized Solar Cells. *ACS Appl. Mater. Interfaces* **2015**, *7*, 3427−3455.

(31) Trost, B. M.; Brittelli, D. R. The Halogenation of Acenaphthene Derivatives. *J. Org. Chem.* **1967**, *32*, 2620−2621.

(32) Majumdar, P.; Mack, J.; Nyokong, T. Synthesis, Characterization and Photophysical Properties of an Acenaphthalene Fused-Ring-Expanded Nir Absorbing Aza-Bodipy Dye. *RSC Adv.* **2015**, *5*, 78253−78258.

(33) Murugesan, V.; de Bettignies, R.; Mercier, R.; Guillerez, S.; Perrin, L. Synthesis and Characterizations of Benzotriazole Based Donor-Acceptor Copolymers for Organic Photovoltaic Applications. *Synth. Met.* **2012**, *162*, 1037−1045.

(34) Chen, Y.; Chou, H.; Tsai, M. C.; Chen, S.; Lin, J. T.; Yao, C.; Chen, K. Thieno[3,4-b]Thiophene-Based Organic Dyes for Dye-Sensitized Solar Cells. *Chem. - Eur. J.* **2012**, *18*, 5430−5437.

(35) Jen, A. K.; Rao, V. P.; Wong, K.; Drost, K. J. Functionalized Thiophenes: Second-Order Nonlinear Optical Materials. *J. Chem. Soc., Chem. Commun.* **1993**, 90−92.

(36) Lin, J. T.; Chen, P. C.; Yen, Y. S.; Hsu, Y. C.; Chou, H. H.; Yeh, M. C. P. Organic Dyes Containing Furan Moiety for High-Performance Dye-Sensitized Solar Cells. *Org. Lett.* **2009**, *11*, 97−100.

(37) Cardona, C. M.; Li, W.; Kaifer, A. E.; Stockdale, D.; Bazan, G. C. Electrochemical Considerations for Determining Absolute Frontier Orbital Energy Levels of Conjugated Polymers for Solar Cell Applications. *Adv. Mater.* **2011**, *23*, 2367−2371.

(38) Fernandes, S. S.; Castro, M. C. R.; Pereira, A. I.; Mendes, A. l.; Serpa, C.; Pina, J.; Justino, L. L.; Burrows, H. D.; Raposo, M. M. M. Optical and Photovoltaic Properties of Thieno[3, 2-b]Thiophene-Based Push−Pull Organic Dyes with Different Anchoring Groups for Dye-Sensitized Solar Cells. *ACS omega* **2017**, *2*, 9268−9279.

(39) Kumaresan, P.; Vegiraju, S.; Ezhumalai, Y.; Yau, S. L.; Kim, C.; Lee, W.-H.; Chen, M.-C. J. P. Fused-Thiophene Based Materials for Organic Photovoltaics and Dye-Sensitized Solar Cells. *Polymers* **2014**, *6*, 2645−2669.

(40) Ji, J. M.; Zhou, H.; Kim, H. K. Rational Design Criteria for D−Π−a Structured Organic and Porphyrin Sensitizers for Highly Efficient Dye-Sensitized Solar Cells. *J. Mater. Chem. A* **2018**, *6*, 14518−14545.

(41) Zhang, H.; Fan, J.; Iqbal, Z.; Kuang, D.-B.; Wang, L.; Cao, D.; Meier, H. J. D. Pigments. *Anti-Recombination Organic Dyes Containing Dendritic Triphenylamine Moieties for High Open-Circuit Voltage of Dsscs* **2013**, *99*, 74−81.

(42) Zhang, L.; Cole, J. M. Dye Aggregation in Dye-Sensitized Solar Cells. *J. Mater. Chem. A* **2017**, *5*, 19541−19559.

(43) Feng, Q. Y.; Zhou, G.; Wang, Z. S. Varied Alkyl Chain Functionalized Organic Dyes for Efficient Dye-Sensitized Solar Cells: Influence of Alkyl Substituent Type on Photovoltaic Properties. *J. Power Sources* **2013**, *239*, 16−23.

(44) Fabian, J. Electronic Excitation of Sulfur-Organic Compounds−Performance of Time-Dependent Density Functional Theory. *J. Theoretical Chemistry Accounts* **2001**, *106*, 199−217.

(45) Williams, D. B. G.; Lawton, M. Drying of Organic Solvents: Quantitative Evaluation of the Efficiency of Several Desiccants. *J. Org. Chem.* **2010**, *75*, 8351−8354.

(46) Still, W. C.; Kahn, M.; Mitra, A. Rapid Chromatographic Technique for Preparative Separations with Moderate Resolution. *J. Org. Chem.* **1978**, *43*, 2923−2925.

(47) Pinto, A. L.; Cruz, L.; Gomes, V.; Cruz, H.; Calogero, G.; de Freitas, V.; Pina, F.; Parola, A. J.; Carlos Lima, J. Catechol Versus Carboxyl Linkage Impact on Dssc Performance of Synthetic Pyranoflavylium Salts. *Dyes Pigments* **2019**, *170*, No. 107577.

(48) Becke, A. D. A New Mixing Off Hartree-Fock and Localdensity-Functional Teories. *J. Chem. Phys.* **1993**, *98*, 1372−1377.

(49) Francl, M. M.; Pietro, W. J.; Hehre, W. J.; Binkley, J. S.; Gordon, M. S.; Defrees, D. J.; Pople, J. A. Self-Consistent Molecular-Orbital Methods 0.23. A Polarization-Type Basis Set for 2nd-Row Elements. *J. Chem. Phys.* **1982**, *77*, 3654−3665.

(50) Casida, M. E. Time-Dependent Density-Functional Response Theory for Molecules: Focus on Functionals. *Abstr. Pap. Am. Chem. Soc.* **1997**, *213*, 271.

(51) Gross, E. K. U.; Kohn, W. Time-Dependent Density-Functional Theory. *Academic Press* **1990**, *21*, 255−291.